Featured in Physics

Moving Crystal Phases of a Quantum Wigner Solid in an Ultra-High-Quality 2D Electron System

P. T. Madathil, ¹ K. A. Villegas Rosales, ¹ Y. J. Chung, ¹ K. W. West, ¹ K. W. Baldwin, ¹ L. N. Pfeiffer, ¹ L. W. Engel, ² and M. Shayegan ⁰ ¹

(Received 4 September 2023; accepted 24 October 2023; published 5 December 2023)

In low-disorder, two-dimensional electron systems (2DESs), the fractional quantum Hall states at very small Landau level fillings (ν) terminate in a Wigner solid (WS) phase, where electrons arrange themselves in a periodic array. The WS is typically pinned by the residual disorder sites and manifests an insulating behavior, with nonlinear current-voltage (I-V) and noise characteristics. We report here measurements on an ultralow-disorder, dilute 2DES, confined to a GaAs quantum well. In the ν < 1/5 range, superimposed on a highly insulating longitudinal resistance, the 2DES exhibits a developing fractional quantum Hall state at ν = 1/7, attesting to its exceptional high quality and dominance of electron-electron interaction in the low filling regime. In the nearby insulating phases, we observe remarkable nonlinear I-V and noise characteristics as a function of increasing current, with current thresholds delineating three distinct phases of the WS: a pinned phase (P1) with very small noise, a second phase (P2) in which dV/dI fluctuates between positive and negative values and is accompanied by very high noise, and a third phase (P3) where dV/dI is nearly constant and small, and noise is about an order of magnitude lower than in P2. In the depinned (P2 and P3) phases, the noise spectrum also reveals well-defined peaks at frequencies that vary linearly with the applied current, suggestive of washboard frequencies. We discuss the data in light of a recent theory that proposes different dynamic phases for a driven WS.

DOI: 10.1103/PhysRevLett.131.236501

Two-dimensional electron systems (2DESs) in a sufficiently strong, perpendicular magnetic field (B) at low temperatures and very small Landau level filling factors $(\nu < 1/5)$ form a many-body ordered array of electrons, known as the quantum Wigner solid (WS) [1-4]. The electrons, having their kinetic energy quenched significantly, succumb to the repulsive Coulomb interaction and form a triangular lattice, maximizing the distance between each pair. In the presence of disorder, the WS breaks into domains and gets pinned to the local disorder sites, which significantly alter the bulk transport properties [5–10]. The longitudinal resistance (R_{xx}) of a pinned WS exhibits an insulating, typically activated behavior, $R_{xx} \propto e^{E_A/2k_BT}$ [11], where E_A is commonly associated with the WS defect formation energy [12-15]. The pinned WS displays microwave- or radio-frequency resonances that can be understood as collective excitations caused by the oscillations of the WS domains within the pinning potential [16,17]. It can also show nonlinear current-voltage (I-V) and noise characteristics, revealing the complex dynamics of a moving WS [9,11,18-24].

While the presence of disorder is a crucial ingredient in the transport properties of a pinned WS, less disordered 2DESs exhibit additional remarkable structure in transport measurements. Recent magnetoresistance measurements in ultrahigh-quality 2DESs [25] indeed show clear signatures of fragile fractional quantum Hall states (FQHSs) at $\nu=1/7$ and other fillings embedded deep within the insulating phase [14], clearly signaling the presence of interaction-driven phenomena at very small fillings. One would expect the quality to be reflected in the WS phase as well and yield novel transport signatures. Our Letter reports striking nonlinear I-V and noise characteristics of the driven WS in this extremely high-quality regime.

The ultrahigh-quality 2DES in our study is realized by confining electrons to an 89-nm-wide GaAs quantum well. The sample was grown using molecular beam epitaxy, following an extensive campaign to improve the crystal purity via an optimization of the growth environment and sample structure [25,26]. The quantum well has flanking $Al_xGa_{1-x}As$ barriers with stepped values of x, and Si dopants inside a doping-well structure [14,25-27]. The very dilute 2DES has an areal density of $\simeq 2.83 \times 10^{10}$ cm⁻² and a record-high mobility of $\simeq 15 \times 10^6$ cm²/V s at such low density. We performed electrical transport measurements on a $4 \times 4 \text{ mm}^2$ van der Pauw geometry, with alloyed In:Sn contacts at its corners and edge midpoints. The sample was cooled in a dilution refrigerator. For details of our measurement protocols, see the Supplemental Material [28].

¹Department of Electrical and Computer Engineering, Princeton University, Princeton, New Jersey 08544, USA
²National High Magnetic Field Laboratory, Florida State University, Tallahassee, Florida 32310, USA

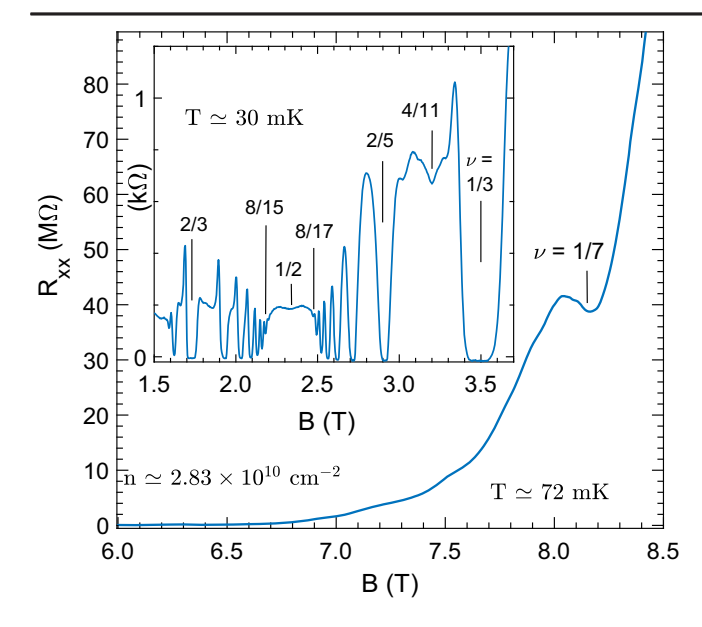


FIG. 1. Longitudinal resistance (R_{xx}) vs magnetic field (B) for a dilute 2DES confined to an 89-nm-wide GaAs quantum well at $T \simeq 72$ mK in the small filling range. The position of an emerging FQHS at $\nu = 1/7$ is marked. Inset: R_{xx} at $T \simeq 30$ mK in the higher filling range.

Figure 1 presents R_{xx} vs B for our 2DES. The sample's exceptionally high quality is evinced from the welldeveloped FQHSs up to $\nu = 8/17$ and $\nu = 8/15$ on the flanks of $\nu = 1/2$ (Fig. 1, inset), as well as an emerging FQHS between $\nu = 1/3$ and 2/5, at $\nu = 4/11$, which can be understood as the FQHS of interacting composite fermions [29–31]. The $\nu = 4/11$ FQHS is extremely fragile and has been reported before only in the highestquality 2DESs and at much higher densities [14,25,32,33]. Its presence in our dilute 2DES is a testament to its unprecedented quality. The data in the high-field range (Fig. 1, main) show that the resistance is approximately 4 orders of magnitude larger than in the low-field trace, indicating a highly insulating behavior when the filling factor is small ($\nu < 1/5$). Nevertheless, we can see a clear R_{xx} minimum at $\nu = 1/7$, strongly corroborating the high quality of this dilute 2DES.

Figure 2(a) displays the nonlinear transport traces at four different temperatures below the melting temperature of the WS, which we deduce to be $T_m \simeq 120$ mK [28,34,35]. We measure the differential resistance (dV/dI) as a function of the driving dc current (I). A small sinusoidal (ac) excitation current of 0.05 nA is superimposed on I, and the ratio of the measured differential voltage to the small signal excitation gives the value of dV/dI. The frequency for the ac current is kept small (0.1 Hz) to maximize the in-phase (resistive) component. The data are obtained at B = 8.40 T ($\nu = 0.139$), past the $\nu = 1/7$ FQHS.

At the lowest T [80 mK, top trace in Fig. 2(a)], dV/dI vs I exhibits a strong nonlinear behavior that can be broken into three distinct regimes, separated by two threshold

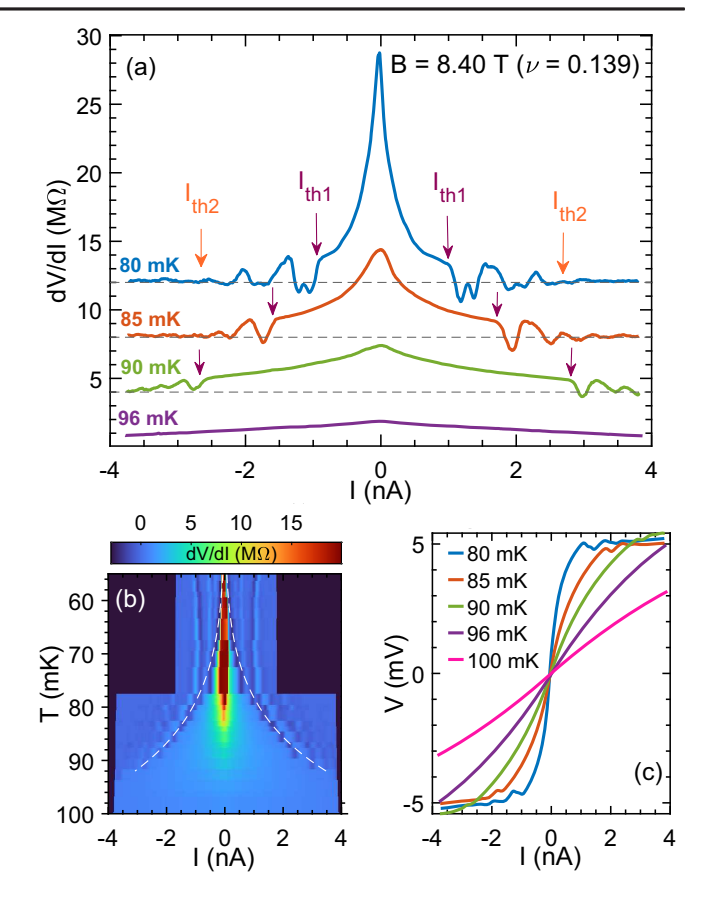


FIG. 2. (a) dV/dI vs I at B=8.40 T ($\nu=0.139$). The different traces, corresponding to different temperatures $T\simeq 80,~85,~90,$ and 96 mK, are offset vertically by 12, 8, 4, and 0 M Ω , respectively. (b) Color-scale plot summarizing dV/dI vs I curves for all temperatures. The dashed white line follows the first minimum corresponding to the negative differential resistance seen just beyond $I_{\rm th1}$. (c) The integrated I-V characteristics at different temperatures.

currents. At very small I, dV/dI drops fairly sharply, by a factor of about 5 within $\simeq 1$ nA, and then shows a very abrupt drop at a first threshold current (I_{th1}) to negative values. We associate I_{th1} with the depinning of the pinned WS. For $I > I_{th1}$, dV/dI becomes nonmonotonic and fluctuates around zero. Beyond a second threshold current (I_{th2}), the amplitude of the fluctuations significantly diminishes, and dV/dI attains a small, relatively constant value, with little dependence on current. We associate the three different regimes separated by I_{th1} and I_{th2} with three different dynamic phases of the WS; we refer to these as P1, P2, and P3, as a function of increasing I, and show later in the Letter that they each possess a distinct noise spectrum.

The traces shown in Fig. 2(a) reveal that the main peak becomes broader and $I_{\rm th1}$ shifts toward higher values as T increases. In addition, the local minima past $I_{\rm th1}$, corresponding to negative dV/dI, become less negative and the amplitude of the fluctuations diminishes until it fully disappears at T=96 mK. Figure 2(b) is a color-scale plot

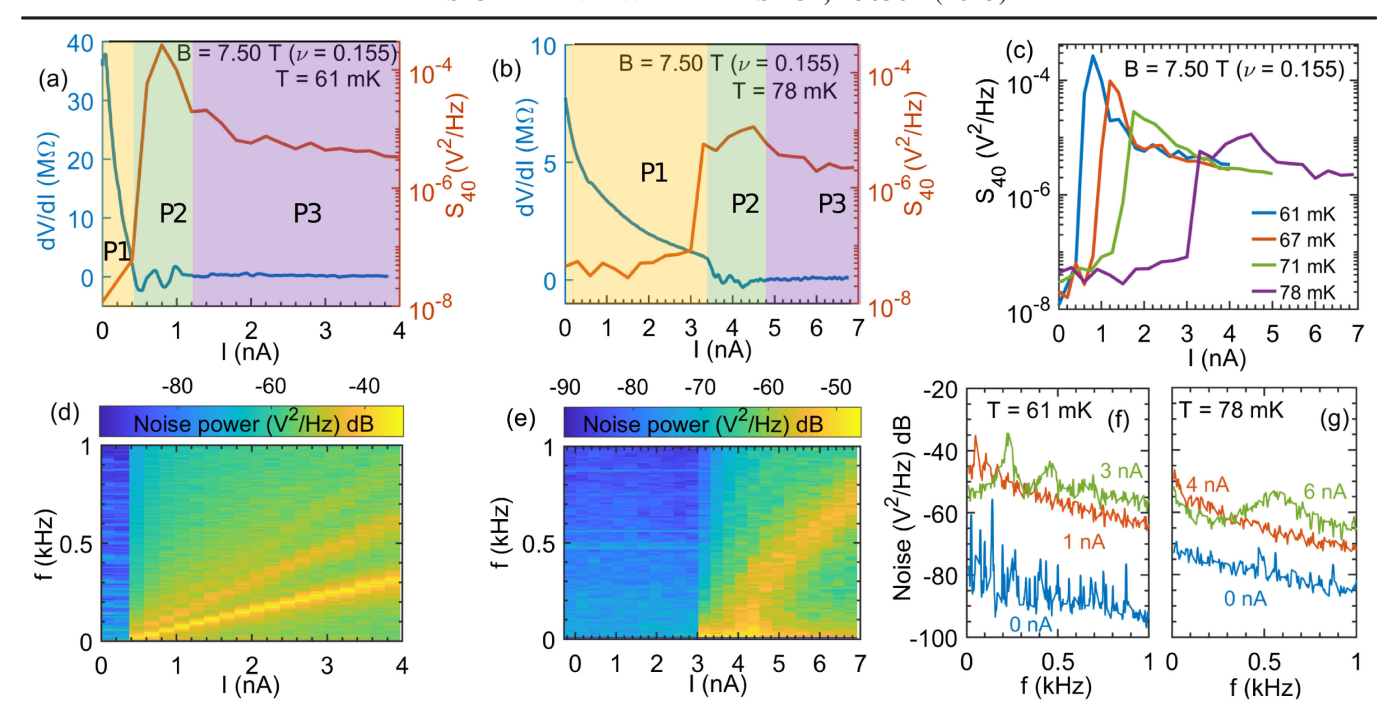


FIG. 3. Noise data at B = 7.50 T ($\nu = 0.155$). (a),(b) dV/dI (blue trace) and noise power obtained by averaging over a frequency window of ± 10 Hz centered at 40 Hz defined as S_{40} (red trace) vs I at $T \simeq 61$ and $\simeq 78$ mK, respectively. (c) S_{40} vs I at different temperatures. The scale for S_{40} is logarithmic and spans over four decades. (d),(e) Color-scale plots summarizing the noise power as a function of f and I at $T \simeq 61$ and $\simeq 78$ mK, respectively. (f),(g) Noise power vs f for different values of I as indicated.

that summarizes dV/dI vs I curves at all temperatures. Figure 2(c) shows the I-V characteristics obtained by integrating the dV/dI vs I curves. At the lowest temperature, I-V is steplike, with a large voltage developed for a small amount of current. This sharp jump can be understood as the voltage, or electric field, required to overcome the pinning potential and cause motion of the WS. Beyond $I_{\text{th}1}$, the voltage fluctuates about the threshold voltage value and increases very gradually with I, indicating that, once depinned, a negligible amount of extra electric field is required to sustain a current. Increasing temperature makes the steplike transitions more smooth, and the fluctuations become weaker, eventually vanishing at the highest temperatures [36].

To further investigate the driven phases of the WS, we measured the noise spectrum in response to a driving dc current, concomitantly with dV/dI. Figure 3 summarizes the noise data at B=7.50 T ($\nu=0.155$). In Fig. 3(a), we show the nonlinear dV/dI (blue trace) together with the noise power averaged between 30 and 50 Hz, defined as S_{40} (red trace) vs I at $T\simeq 61$ mK. Qualitatively similar to Fig. 2(a) data, the dV/dI vs I data in Fig. 3(a) exhibit two current thresholds that delineate three phases. [Note that the data in Figs. 2(a) and 3(a) were taken at different fillings and temperatures.] There is a remarkable correlation between the behaviors of S_{40} and dV/dI with I in Fig. 3(a) in the three phases. At low drives ($I < I_{th1} \simeq 0.4$ nA), the noise is low ($S_{40} < 10^{-7}$ V²/Hz). We identify this pinned, lownoise phase as P1. For currents between I_{th1} and I_{th2}

 $(0.4 \lesssim I \lesssim 1.2 \text{ nA})$, where dV/dI fluctuates, S_{40} rises dramatically, by about 4 orders of magnitude, and reaches a peak value of $\simeq 10^{-4} \text{ V}^2/\text{Hz}$. This is the second phase, P2. Past P2, in phase P3, dV/dI is very low and constant, noise decreases and, for large driving currents ($I \gtrsim 2 \text{ nA}$), it becomes roughly constant and settles at a value of $\simeq 3 \times 10^{-6} \text{ V}^2/\text{Hz}$.

In Fig. 3(b), we present nonlinear dV/dI and S_{40} data at a higher temperature of $T \simeq 78$ mK. The dV/dI trace indicates larger threshold currents, with suppressed fluctuating dV/dI features in the P2 phase. The latter is also reflected in S_{40} data, where the peak in S_{40} in phase P2 is strongly suppressed compared to Fig. 3(a) data. Data shown in Fig. 3(c) at intermediate temperatures display the evolution of S_{40} with temperature.

In addition to S_{40} , we also measured the noise power spectrum between 5 Hz and 1 kHz as a function of frequency (f) at different driving currents. Figure 3(f) contains such data at $T \simeq 61$ mK, for I=0,1, and 3 nA. A summary of the full noise response vs f and I at $T \simeq 61$ mK is presented as a color-scale plot in Fig. 3(d). The noise spectrum reveals a distinct peak, accompanied by additional harmonics, that shift to higher frequencies with increasing I in the P2 and P3 phases. The peak frequencies are linear in I, consistent with a signal that is of the washboard type [37]. However, the frequency values we observe are $\sim 10^3$ times smaller than the expected washboard frequencies estimated from the expression $f = J/nea_0$ where J is the current density, n is the electron density, e is the electron charge, and e0 is the WS

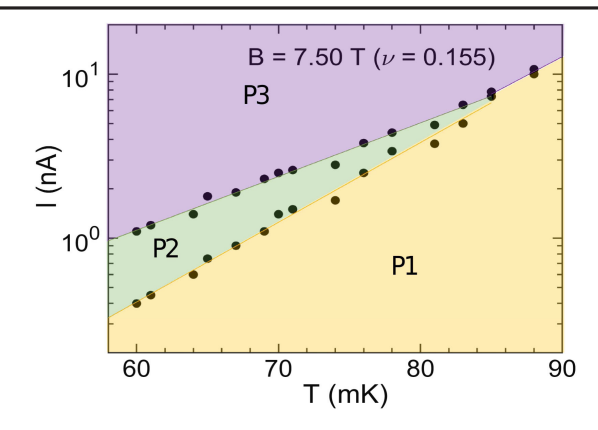


FIG. 4. Phase diagram for the WS as a function of T and I at B = 7.50 T ($\nu = 0.155$).

lattice constant [22,37]. Figure 3(g) contains the noise response vs f at a higher temperature of $T \simeq 78$ mK, for I=0, 4, and 6 nA. A summarized color-scale plot is presented in Fig. 3(e). At this higher temperature, only a broad peak is observed for I=6 nA. In the Supplemental Material [28], we report the temperature dependence of the slope of the f vs I plots [see Figs. 3(d) and 3(e)] and of the power associated with the fundamental frequency of the narrow band noise spectra.

Our experimental observations can be summarized in a phase diagram for the WS as presented in Fig. 4. The data are taken at $B=7.50~\mathrm{T}~(\nu=0.155)$, and I is presented in a log scale to visualize the width of the P2 region clearly. The black data points are obtained from the two thresholds, $I_{\mathrm{th}1}$ and $I_{\mathrm{th}2}$, extracted from dV/dI vs I data. The extent of the P2 phase in I is widest at the lowest temperatures. It narrows as T increases and completely disappears above $T\simeq85~\mathrm{mK}$ (see Supplemental Material [28] for dV/dI and S_{40} data at $T\simeq85~\mathrm{mK}$).

Our observations of noise and the dV/dI data follow closely the numerical calculations of Reichhardt et al. [38-40], which suggest the presence of a pinned phase, followed by a moving WS glass phase, and then a moving smectic phase, with increasing drive. At low temperatures, below the melting temperature of the WS, the disordered WS exhibits channel flow just above the first threshold. In this phase, the conduction is filamentary and can show jumps in dV/dI that can be negative [38–40]. Our dV/dI data also show fluctuations, with negative dV/dIjust above depinning, which disappears at $T \simeq 85$ mK. Note that $T_m \simeq 120$ mK for the WS in our sample [28], and thus the P2 phase is lost before the WS melts. Our experimental observation of fluctuating and negative dV/dI in phase P2 is highly suggestive of the filamentary phase reported in Refs. [39,40].

Reichhardt and Reichhardt [39,40] also report on noise power (which we associate with S_{40} in our Letter) as a function of the drive. Their calculations show suppressed noise in the pinned phase, high noise in the moving glass phase, and low noise in the moving smectic phase as

the drive increases. Our S_{40} data also reveal a similar qualitative picture, with S_{40} being very low in phase P1, high in phase P2, and suppressed again in phase P3, with increasing current.

Despite the above qualitative agreements, there are some notable departures. While theory [39,40] predicts the emergence of the washboard signal only in the P3 (moving smectic) phase, we observe the noise peaks in phases P2 and P3. Also, although the linear dependence of the peak frequency on I that we observe [Fig. 3(d)] is consistent with the washboard frequency, the 3 orders of magnitude discrepancy between the experimental and estimated frequencies is puzzling and leaves room for speculation. One possibility is that the origin of the noise signal is the motion of WS domains and its interaction with the disorder potential. If we assume that the domains have a reasonably uniform size, and since the domain size is much larger than the WS lattice constant, the resulting peak frequencies can be much smaller than the washboard frequency [41]. Based on our observed $E_{th} \simeq 1 \text{ V/m}$, and the expression $L_0^2 \simeq 0.02e/4\pi\epsilon\epsilon_0 E_{\rm th}$ [42], we obtain a rough estimate of $nL_0^2 \simeq 600$ electrons/domain [43–46]. It is worth mentioning that narrow band noise peaks have been reported in the reentrant integer quantum Hall states, and there too, the observed frequencies are much smaller than the expected washboard value [47,48]. In the Supplemental Material [28], we also report voltage (V) vs time (t) traces of the noise measured with an oscilloscope. The real-time waveforms are sawtoothlike, suggesting a stick-slip motion of the domains as they encounter disorder sites [49,50].

There have been previous experiments reporting the nonlinear I-V and noise characteristics of the high-field ($\nu < 1/5$) WSs [11,18–21,24]. While the data presented in these studies have distinct dissimilarities, a common conclusion has been the existence of two phases, a pinned phase at low drives, followed by a sliding phase at high drives. In our ultrahigh-quality samples, we report an additional phase where dV/dI is negative and fluctuating and is accompanied by a large, low-frequency noise [Fig. 3(c)]. This is different from the data in previous work, as is the presence of a current-dependent peak in the noise spectrum in the depinned phases [Figs. 3(d) and 3(e)] [51].

We also note that a rich collection of experiments on the negative dV/dI exists in different platforms, suggesting a variety of possible mechanisms. In Refs. [52–54], e.g., transport measurements of classical WSs formed on the surface of superfluid helium at zero magnetic field are reported. Reference [55] reports two-threshold *I-V* characteristics past the metal-insulator transition in Si-MOSFETs. While the phenomena reported in Refs. [52–55] happen in the insulating phases, a more surprising observation is the similarity of our *I-V* features to those reported in Ref. [56] in a GaAs 2DES, but in vastly different parameter ranges: \sim 30 times larger density, \sim 100 times higher temperatures, \sim 10 000 times larger currents, and \sim 10 times lower magnetic

fields ($B \sim 0.8$ T, $\nu \sim 50$). The I-V characteristics were attributed to a redistribution of electrons in energy space, induced by the current [56]. These observations highlight the complexities and yet certain qualitative similarities of the electrical transport properties in remarkably different platforms and circumstances. Finally, it has been theoretically proposed that composite fermion correlations present in the FQHSs persist in the WS phase and that composite fermion WSs are more stable than electron WSs at very low fillings [13,57]. Our data presented here should prove useful in testing future theories dealing with the transport characteristics of composite fermion WSs.

We thank S. A. Lyon for loaning us the HP-3562A spectrum analyzer, as well as D. A. Huse and J. K. Jain for illuminating discussions. We acknowledge support by the National Science Foundation (NSF) Grant No. DMR 2104771 for measurements. For sample characterization, we acknowledge support by the U.S. Department of Energy Basic Energy Office of Science, Basic Energy Sciences (Award No. DEFG02-00-ER45841) and, for sample synthesis, NSF Grant No. ECCS 1906253 and the Gordon and Betty Moore Foundation's EPiQS Initiative (Grant No. GBMF9615 to L. N. P.).

- [1] E. Wigner, On the interaction of electrons in metals, Phys. Rev. **46**, 1002 (1934).
- [2] P. K. Lam and S. M. Girvin, Liquid-solid transition and the fractional quantum-Hall effect, Phys. Rev. B **30**, 473 (1984).
- [3] D. Levesque, J. J. Weis, and A. H. MacDonald, Crystallization of the incompressible quantum-fluid state of a two-dimensional electron gas in a strong magnetic field, Phys. Rev. B **30**, 1056 (1984).
- [4] H. Yi and H. A. Fertig, Laughlin-Jastrow-correlated Wigner crystal in a strong magnetic field, Phys. Rev. B 58, 4019 (1998).
- [5] D. S. Fisher, B. I. Halperin, and R. Morf, Defects in the twodimensional electron solid and implications for melting, Phys. Rev. B 20, 4692 (1979).
- [6] I. M. Ruzin, S. Marianer, and B. I. Shklovskii, Pinning of a two-dimensional Wigner crystal by charged impurities, Phys. Rev. B 46, 3999 (1992).
- [7] Min-Chul Cha and H. A. Fertig, Orientational order and depinning of the disordered electron solid, Phys. Rev. Lett. **73**, 870 (1994).
- [8] X. Zhu, P. B. Littlewood, and A. J. Millis, Sliding motion of a two-dimensional Wigner crystal in a strong magnetic field, Phys. Rev. B 50, 4600 (1994).
- [9] For an early review, see M. Shayegan, in *Perspectives in Quantum Hall Effects*, edited by S. D. Sarma and A. Pinczuk (Wiley, New York, 1997), pp. 343–383.
- [10] R. Chitra, T. Giamarchi, and P. Le Doussal, Dynamical properties of the pinned Wigner crystal, Phys. Rev. Lett. 80, 3827 (1998).
- [11] H. W. Jiang, H. L. Stormer, D. C. Tsui, L. N. Pfeiffer, and K. W. West, Magnetotransport studies of the insulating

- phase around $\nu = 1/5$ Landau-level filling, Phys. Rev. B **44**, 8107 (1991).
- [12] R. Narevich, G. Murthy, and H. A. Fertig, Hamiltonian theory of the composite-fermion Wigner crystal, Phys. Rev. B 64, 245326 (2001).
- [13] A. C. Archer and J. K. Jain, Quantum bubble defects in the lowest-Landau-level crystal, Phys. Rev. B 90, 201309(R) (2014).
- [14] Yoon Jang Chung, D. Graf, L. W. Engel, K. A. Villegas Rosales, P. T. Madathil, K. W. Baldwin, K. W. West, L. N. Pfeiffer, and M. Shayegan, Correlated states of 2D electrons near the Landau level filling $\nu=1/7$, Phys. Rev. Lett. **128**, 026802 (2022).
- [15] P. T. Madathil, C. Wang, S. K. Singh, A. Gupta, K. A. Villegas Rosales, Y. J. Chung, K. W. West, K. W. Baldwin, L. N. Pfeiffer, L. W. Engel, and M. Shayegan (unpublished).
- [16] E. Y. Andrei, G. Deville, D. C. Glattli, F. I. B. Williams, E. Paris, and B. Etienne, Observation of a magnetically induced Wigner solid, Phys. Rev. Lett. **60**, 2765 (1988).
- [17] Y. P. Chen, G. Sambandamurthy, Z. H. Wang, R. M. Lewis, L. W. Engel, D. C. Tsui, P. D. Ye, L. N. Pfeiffer, and K. W. West, Melting of a 2D quantum electron solid in high magnetic field, Nat. Phys. 2, 452 (2006).
- [18] R. L. Willett, H. L. Stormer, D. C. Tsui, L. N. Pfeiffer, K. W. West, M. Shayegan, M. Santos, and T. Sajoto, Current-voltage discontinuities in high-quality two-dimensional electron systems at low Landau-level filling factors, Phys. Rev. B 40, 6432 (1989).
- [19] V. J. Goldman, M Santos, M Shayegan, and J. E. Cunningham, Evidence for two-dimensional quantum Wigner crystal, Phys. Rev. Lett. 65, 2189 (1990).
- [20] F. I. B. Williams, P. A. Wright, R. G. Clark, E. Y. Andrei, G. Deville, D. C. Glattli, O. Probst, B. Etienne, C. Dorin, C. T. Foxon, and J. J. Harris, Conduction threshold and pinning frequency of magnetically induced Wigner solid, Phys. Rev. Lett. 66, 3285 (1991).
- [21] Yuan P. Li, T. Sajoto, L. W. Engel, D. C. Tsui, and M. Shayegan, Low-frequency noise in the reentrant insulating phase around the 1/5 fractional quantum Hall liquid, Phys. Rev. Lett. **67**, 1630 (1991).
- [22] Yuan P. Li, D. C. Tsui, L. W. Engel, M. B. Santos, T. Sajoto, and M. Shayegan, RF resonance in two-dimensional electron transport in the Wigner solid regime, Solid State Commun. **96**, 379 (1995).
- [23] Yuan P. Li, D. C. Tsui, L. W. Engel, M. B. Santos, and M. Shayegan, Inductive anomaly of two-dimensional electrons in the Wigner solid regime, Solid State Commun. 99, 255 (1996).
- [24] G. A. Csáthy, D. C. Tsui, L. N. Pfeiffer, and K. W. West, Astability and negative differential resistance of the Wigner solid, Phys. Rev. Lett. 98, 066805 (2007).
- [25] Yoon Jang Chung, K. A. Villegas Rosales, K. W. Baldwin, P. T. Madathil, K. W. West, M. Shayegan, and L. N. Pfeiffer, Ultra-high-quality two-dimensional electron systems, Nat. Mater. 20, 632 (2021).
- [26] Yoon Jang Chung, A. Gupta, K. W. Baldwin, K. W. West, M. Shayegan, and L. N. Pfeiffer, Understanding limits to mobility in ultrahigh-mobility GaAs two-dimensional electron systems: 100 million cm²/Vs and beyond, Phys. Rev. B 106, 075134 (2022).

- [27] Yoon Jang Chung, K. A. Villegas Rosales, K. W. Baldwin, K. W. West, M. Shayegan, and L. N. Pfeiffer, Working principles of doping-well structures for high-mobility twodimensional electron systems, Phys. Rev. Mater. 4, 044003 (2020).
- [28] See Supplemental Material at http://link.aps.org/ supplemental/10.1103/PhysRevLett.131.236501 for additional measurements and analysis.
- [29] Arkadiusz Wójs and John J. Quinn, Quasiparticle interactions in fractional quantum Hall systems: Justification of different hierarchy schemes, Phys. Rev. B 61, 2846 (2000).
- [30] Arkadiusz Wójs, Kyung-Soo Yi, and John J. Quinn, Fractional quantum Hall states of clustered composite fermions, Phys. Rev. B 69, 205322 (2004).
- [31] Sutirtha Mukherjee, Sudhansu S. Mandal, Ying-Hai Wu, Arkadiusz Wójs, and Jainendra K. Jain, Enigmatic 4/11 state: A prototype for unconventional fractional quantum Hall effect, Phys. Rev. Lett. **112**, 016801 (2014).
- [32] W. Pan, K. W. Baldwin, K. W. West, L. N. Pfeiffer, and D. C. Tsui, Fractional quantum Hall effect at Landau level filling $\nu = 4/11$, Phys. Rev. B **91**, 041301(R) (2015).
- [33] N. Samkharadze, I. Arnold, L. N. Pfeiffer, K. W. West, and G. A. Csáthy, Observation of incompressibility at $\nu = 4/11$ and $\nu = 5/13$, Phys. Rev. B **91**, 081109(R) (2015).
- [34] Our deduced melting temperature is consistent with the melting phase diagram reported in [35].
- [35] H. Deng, L. N. Pfeiffer, K. W. West, K. W. Baldwin, L. W. Engel, and M. Shayegan, Probing the melting of a two-dimensional quantum Wigner crystal via its screening efficiency, Phys. Rev. Lett. **122**, 116601 (2019).
- [36] It is worth noting that, while the current threshold $I_{\text{th}1}$ increases with increasing temperature, the voltage threshold remains approximately fixed at \simeq 5 mV [see Fig. 2(c)].
- [37] G. Grüner, The dynamics of charge-density waves, Rev. Mod. Phys. **60**, 1129 (1988).
- [38] C. Reichhardt, C. J. Olson, N. Grønbech-Jensen, and Franco Nori, Moving Wigner glasses and smectics: Dynamics of disordered Wigner crystals, Phys. Rev. Lett. 86, 4354 (2001).
- [39] C. Reichhardt and C. J. O. Reichhardt, Nonlinear dynamics, avalanches, and noise for driven Wigner crystals, Phys. Rev. B **106**, 235417 (2022).
- [40] C. Reichhardt and C. J. O. Reichhardt, Noise and thermal depinning of Wigner crystals, J. Phys. Condens. Matter 35, 325603 (2023).
- [41] P. Monceau, Electronic crystals: An experimental overview, Adv. Phys. 61, 325 (2012).
- [42] H. Fukuyama and P. A. Lee, Dynamics of the charge-density wave. I. Impurity pinning in a single chain, Phys. Rev. B 17, 535 (1978).
- [43] Our estimate of the WS domain size, $L_0 \simeq 1.5 \, \mu m$, is consistent with the recent results of microwave measurements [44,45] where WS pinning mode resonances at very small frequencies ($\simeq 30 \, \text{MHz}$) are observed in ultrahigh-quality samples similar to ours. These are the smallest pinning mode resonance frequencies reported for magnetic-field-induced WSs and attest to the exceptionally high quality of the samples.
- [44] Lili Zhao, Wenlu Lin, Yoon Jang Chung, Adbhut Gupta, Kirk W. Baldwin, Loren N. Pfeiffer, and Yang Liu, Dynamic

- response of Wigner crystals, Phys. Rev. Lett. **130**, 246401 (2023).
- [45] Matthew L. Freeman, P. T. Madathil, L. N. Pfeiffer, K. W. Baldwin, Y. J. Chung, L. W. Engel, R. Winkler, and M. Shayegan (unpublished).
- [46] We also obtain the activation energies (E_A) by measuring the temperature dependence of R_{xx} in the filling factor range $6 \lesssim 1/\nu \lesssim 7$ using the expression $R_{xx} \propto e^{E_A/2k_BT}$. We report $E_A \simeq 2$ K for our sample [14]. This is two times larger than the values reported previously for samples with similar densities but of lower quality. It is close to the theoretically calculated E_A for defect energies in a clean WS [13], reflecting the extremely high quality and large domains of the WS realized in our system.
- [47] K. B. Cooper, J. P. Eisenstein, L. N. Pfeiffer, and K. W. West, Observation of narrow-band noise accompanying the breakdown of insulating states in high Landau levels, Phys. Rev. Lett. 90, 226803 (2003).
- [48] Jian Sun, Jiasen Niu, Yifan Li, Yang Liu, L. N. Pfeiffer, K. W. West, Pengjie Wang, and Xi Lin, Dynamic ordering transitions in charged solid, Fundam. Res. 2, 178 (2022).
- [49] G. Grüner, *Density Waves in Solids* (Perseus, Cambridge, MA, 1994).
- [50] Tomoyuki Sekine, Norikazu Satoh, Mitsuhiro Nakazawa, and Toshikazu Nakamura, Sliding spin-density wave in (TMTSF)₂PF₆ studied with narrow-band noise, Phys. Rev. B **70**, 214201 (2004).
- [51] While a negative dV/dI and frequency-dependent noise in WS was reported in Ref. [24], the negative dV/dI regime was devoid of any fluctuations, and the noise peak in the spectra was restricted only to the negative dV/dI regime. The frequency-dependent noise in our experiments extends well beyond the negative and fluctuating dV/dI regime and into the P3 phase, clearly differentiating our data in this new, ultrahigh-quality 2DES.
- [52] P. Glasson, V. Dotsenko, P. Fozooni, M. J. Lea, W. Bailey, G. Papageorgiou, S. E. Andresen, and A. Kristensen, Observation of dynamical ordering in a confined Wigner crystal, Phys. Rev. Lett. 87, 176802 (2001).
- [53] David G. Rees, Niyaz R. Beysengulov, Juhn-Jong Lin, and Kimitoshi Kono, Stick-slip motion of the Wigner solid on liquid helium, Phys. Rev. Lett. **116**, 206801 (2016).
- [54] Shan Zou, Denis Konstantinov, and David G. Rees, Dynamical ordering in a two-dimensional electron crystal confined in a narrow channel geometry, Phys. Rev. B 104, 045427 (2021).
- [55] Pedro Brussarski, S. Li, S. V. Kravchenko, A. A. Shashkin, and M. P. Sarachik, Transport evidence for a sliding twodimensional quantum electron solid, Nat. Commun. 9, 3803 (2018).
- [56] A. A. Bykov, Jing-qiao Zhang, Sergey Vitkalov, A. K. Kalagin, and A. K. Bakarov, Zero-differential resistance state of two-dimensional electron systems in strong magnetic fields, Phys. Rev. Lett. 99, 116801 (2007).
- [57] A. C. Archer, K. Park, and J. K. Jain, Competing crystal phases in the lowest Landau level, Phys. Rev. Lett. **111**, 146804 (2013).